King Saud University

Arabian Journal of Chemistry

www.ksu.edu.sa
www.sciencedirect.com

ORIGINAL ARTICLE

Study of the activity and stability of sulfonated carbon catalyst from agroindustrial waste in biodiesel production: Influence of pyrolysis temperature on functionalization

Ana Paula da Luz Corrêa, Paula Maria Melo da Silva, Matheus Arrais Gonçalves, Rafael Roberto Cardoso Bastos, Geraldo Narciso da Rocha Filho, Leyvison Rafael Vieira da Conceição *

Federal University of Pará, Institute of Exact and Natural Sciences, Graduate in Chemistry Program, Laboratory of Catalysis and Oleochemical, 66075–110 Belém, Pará, Brazil

Abstract   The influence of pyrolysis temperature on the activity and catalytic stability of sulfonated biochar, from the agro-industrial residue murumuru kernel shell, was evaluated in the esterification reaction. Carbonaceous materials were synthesized by direct pyrolysis at 450, 600 and 750 °C and functionalized with sulfuric acid at 200 °C for a 4 h period. The materials were characterized by density of sulfonic groups, SEM, EDS, Elementary Analysis, ATR-FTIR, Raman Spectroscopy, TG and XPS analysis. The data obtained showed that the functionalization occurred directly in the carbon chain of biochar, evidencing that higher carbonization temperatures resulted in carbonaceous catalysts of more stable polycondensed nature. The catalyst synthesized at 750 °C achieved conversion of 98.35% ± 1.105 and maintained in the third reaction cycle conversion of 89.35% ± 1.197. This catalyst also showed the highest content of sulfur groups, even after reuse processes. The increment of temperature and time in the reaction medium was able to improve the reuse capacity of relatively low stability catalysts. Thus, the results obtained show the impact of pyrolysis temperature on obtaining catalysts with greater activity and catalytic stability in esterification reactions, and in this way provide very important subsidies for the development of new heterogeneous sulfonated carbon-based catalysts, applied in the biodiesel production process.

© 2023 The Author(s). Published by Elsevier B.V. on behalf of King Saud University. This is an open access article under the CC BY-NC-ND license (http://creativecommons.org/licenses/by-nc-nd/4.0/).

* Corresponding author.
  E-mail address: rafaelvieira@ufpa.br (L.R.V. da Conceição).

1. Introduction

Global concerns regarding fossil fuel consumption and its impact on the environment have led to the implementation of renewable energy policies worldwide, with emphasis on ethanol and biodiesel production (Acharya and Perez-Pena, 2020). Biodiesel is a biodegradable fuel of a non-toxic nature, which has similar performance to petroleum-derived diesel, and can be produced by esterification and transesterification reactions of vegetable oils or animal fats with a low molecular weight alcohol (Gardy et al., 2017; Wee et al., 2019).

The use of heterogeneous acid catalysts is highlighted in the biodiesel production process, because in addition to allowing the occurrence of simultaneous esterification-transesterification reactions, it has the advantages of non-corrosiveness, ease separation and possibility to reuse the solid catalyst. Thus, such materials are an alternative for reactions using low-cost raw material with high acidity (Dechakhumwat et al., 2020; Deris et al., 2020; Zhou et al., 2016). Among the different types of heterogeneous catalysts, carbon-based catalysts have been studied in biodiesel production. These could be derived from a variety of precursors, including biomass residues (Thushari and Babel, 2018).

In recent years, the potential of waste materials has been widely explored with the aim of identifying strategies to convert low-value waste into new materials (Xu et al., 2019). Several types of biochemical and agrochemical processes are being perfected to explore the conversion of agroindustrial waste into products with high added value, such as the production of antifungals and biopigments (Schalchli et al., 2021), production of cellulose acetate (Battisti et al., 2018) and development of biomortars (Boumaaza et al., 2023). Among the different applications, the systematic conversion of biomass residues into compounds such as biochar through pyrolysis techniques is a promising alternative to minimize the environment pollution and ensure the establishment of the bioeconomy (Ghodake et al., 2021).

The use of these residues for the synthesis of heterogeneous catalysts, combined with the use of raw materials with high fatty acid content in biodiesel production can lead to a more economical and sustainable process (Thushari and Babel, 2018).

An important step in the synthesis process of carbonaceous catalysts is pyrolysis of biomass, followed by functionalization with groups that give it catalytic activity. The surface of the biochar has abundant functional groups that could be modified with several other groups after functionalization (Chellappan et al., 2019). Among them, the sulfonated biochar with sulfonic groups ($-SO_3H$) is the most used (Dhawane et al., 2018). The literature reports that the insertion of sulfonic groups in the structure of carbonaceous materials can occur in the benzene groups of the carbon chain, forming sulfonic groups, or in the hydroxyl groups, producing the organo-sulfate groups (Landwehr et al., 2018).

Chemical reactions and physical changes during biomass pyrolysis depend on several factors such as reactor type, heating rate, temperature and biomass composition. Pyrolysis temperature strongly influences the molecular structure and physical–chemical properties of biochar materials. However, more detailed studies on the influence of the temperature of the pyrolysis process on the characteristics and applicability of biochar are necessary to infer and improve preliminary ideas and conclusions, mainly related to the functionalization of sulfonated biochars (Ghodake et al., 2021).

Several studies report the synthesis of sulfonated biochar catalysts applied in esterification reactions, which present high catalytic activity, however they encounter difficulties in the reuse process of the catalyst (Zhou et al., 2016; Lathiya et al., 2018; Niu et al., 2018).

Sulfonated carbon materials exhibit high thermal stability (close to 250 °C), however the real stability of the material and particularly the stability of active sites ($-SO_3H$) is affected by operational or process conditions. Reaction parameters such as temperature, pressure, nature of reagents, pH, presence of solvents and water have a direct impact on the stability of such catalysts. The stability of $-SO_3H$ groups is also influenced by the sulfonation method and the structure of the carbonized material (Chen et al., 2019; Fraile et al., 2015; Scholz et al., 2018). In this context, the literature has few studies to elucidate issues related to the catalytic activity and stability of sulfonated biochar (Chen et al., 2019; Scholz et al., 2018).

The main experimental variables that affect biodiesel yield in esterification and transesterification reactions are the amount of catalyst, the molar ratio between alcohol and raw material, reaction time and temperature. Reaction temperature is usually the factor of greatest influence (Bastos et al., 2020; Gonçalves et al., 2021; Mares et al., 2021). Factorial planning is a very relevant tool to investigate the influence of reaction variables on the biodiesel production process, since it allows identifying the most important factor, evaluating the interactions between variables, predicting responses to conditions that have not been tested in practice and minimizing waste generation with unnecessary experiments (Pereira Filho, 2018).

The Murumuru (*Astrocaryum murumuru* Mart.) is a palm tree of medium height, found throughout the estuary of the Amazon River and tributaries. The fruit pit has a woody shell, containing a kernel that is raw material for the extraction of butter, of high added value in cosmetic formulations. The kernel shell represents an agro-industrial residue with poorly exploited reuse potential (Pesce, 2009; Sousa et al., 2004). Studies have already been developed on the use of this residue for the synthesis of sulfonated carbon catalyst applied in esterification reaction and transesterification of acid oils for biodiesel production (Bastos et al., 2020; Corrêa et al., 2020). However, any study focused on investigating the catalytic activity and stability of this material. Therefore, the present work seeks to investigate the influence of pyrolysis temperature on the synthesis of sulfonated biochar from murumuru kernel regarding catalytic activity and stability in the esterification reaction of oleic acid with methanol, as well as to evaluate the influence of reaction conditions for catalysts with different stabilities.

2. Materials and method

2.1. Materials

The agro-industrial residue of murumuru kernel shell was obtained from the vegetable oil processing company Beraca Ingredientes Naturais S/A located in Ananindeua (Pará, Brazil). In the sulfonation process, 98% concentrated sulfuric acid was used (Exodus®, 7664-93-9). For esterification reactions, 99.8% methanol (Nuclear®, 67-56-1) and oleic acid 99% (Impex®, 112-80-1) were used. Ethanol 99.8% (Êxodo®, 64-17-5) and n-hexane 95% (Vetec®, 110-54-3) were used in the catalyst recovery (washing) process. All reagents used were analytical grade.

2.2. Synthesis of catalysts

The murumuru kernel shell was initially crushed, followed by granulometric classification. The grains of the shell with particle size $\geq$ 340 μm were carbonized in a tubular furnace at temperatures of 450 °C, 600 °C and 750 °C for 1 h, heating rate of 15 °C min^{-1} and nitrogen flow of 80 mL min^{-1}. The conditions used in the pyrolysis process were adapted from the study of Corrêa et al. (2020). The biochars obtained from the different carbonization temperatures were labeled BC450, BC600 and BC750, in which the numbering refers to the carbonization temperature. The Fig. 1a illustrates the synthesis process of biochars. After carbonization, the materials were macerated in gral and pistil. Then, the mass yield of the carbonization of murumuru kernel shell residue was calculated at the different temperatures used.
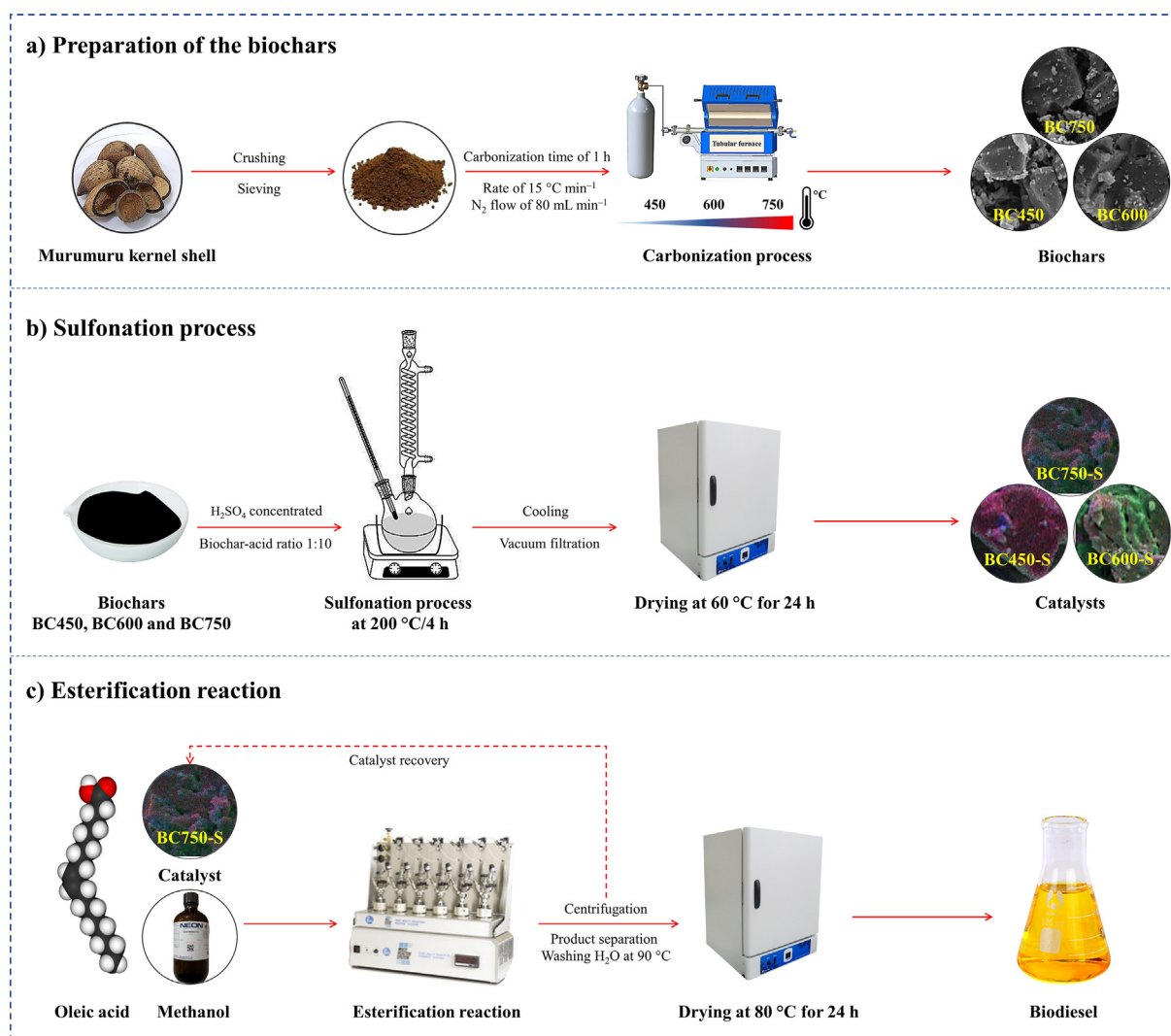
Fig. 1 Flowchart of synthesis and application of catalysts in biodiesel production.

Then, the biochars were functionalized by means of sulfonation process with concentrated sulfuric acid, using a solid-acid ratio 1:10 (1.0 g of biochar for 10 mL of H_2SO_4), in a flat bottom glass balloon and heating plate under constant agitation at 200 °C for a 4 h time period, in reflux system (Corrêa et al., 2020). After the sulfonation stage, the reaction mixture was cooled to room temperature. Afterwards, 500 mL of deionized water was slowly added to the flask in order to dilute the reaction medium. Subsequently, the solid was filtered with filter paper in a vacuum system, washed with deionized water to neutral pH and dried in an oven at 60 °C for 24 h, obtaining sulfonated biochar catalysts labeled BC450-S, BC600-S and BC750-S, in which the term ''S'' refers to the sulfonation process. This functionalization process can be visualized in Fig. 1b.

2.3. Characterization of materials

The density of sulfonic groups was determined by acid-base titration, according to the method proposed by Ning and Niu. (2017), with adaptations. The mass of 0.05 g of the mate-

rial was added in 15 mL of standard NaCl 2.0 mol L^{-1} solution, kept under agitation for 24 h. After that, the suspension was vacuum filtered using quantitative filter paper for solids separation and the filtrate was titrated with standard NaOH solution 0.02 mol L^{-1}, using phenolphthalein as an indicator. The density of the sulfonic groups was calculated according to Eq. (1).

$$C(-SO_3H) = \frac{COH^- x \Delta V}{m} \qquad (1)$$

where C $(-SO_3H)$ is the density of sulfonic groups in mmol g^{-1}; COH^- is the concentration of the standard NaOH solution in mol L^{-1}; ΔV is the Volume of NaOH used for titration in mL; and m is the mass of the sample in g.

The morphological analysis of biochars and catalysts was performed by Scanning Electron Microscopy (SEM), using a high resolution microscope of the TESCAN brand, model VEGA 3 LMU. The characterization of the chemical composition was performed by X-ray Spectroscopy by Dispersion in Energy (EDS), using a micro-analysis system equipment, model AZTec Energy X-Act, with resolution of 129 Ev from Oxford brand. The Elemental Analysis of the materials was

performed in an Element Analyzer equipment, Thermo Scientific brand, model Fisons EA1108 CHNS-O, which allowed the determination of carbon, hydrogen, nitrogen and sulfur percentages. The oxygen content was determined by difference in the sum of C, H, N and S elements. At the end, the atomic ratios H/C and O/C were calculated.

The functional groups present in biochars and catalysts were determined at room temperature by Attenuated Total Reflectance Fourier Transform Infrared Spectroscopy (ATR-FTIR) using a Bruker spectrometer, model VERTEX 70 V equipped with a single-reflection ATR accessory (Platinum, Bruker Optics), recording in the spectral range from 4000 to 400 cm^{-1} with a resolution of 4 cm^{-1}, accumulating 32 scans per spectra. The Raman spectra of biochars and catalysts were obtained using a LabRaM HR spectrometer from Horiba, equipped with a Czerny-Turner monochromator, a CCD detector and an Olympus confocal microscope, operating with a 532 nm laser and 50x lens.

The Thermogravimetric Analysis (TG) of biochars and their respective catalysts was performed in Shimadzu equipment, model DTG-60H, in the temperature range of 25 °C to 1000 °C at a heating rate of 15 °C min^{-1} under nitrogen atmosphere, flow rate 50 mL min^{-1}, using an alumina crucible. The investigation of the chemical speciation of the functional groups present on the surface of the catalysts was performed by X-ray Photoelectron Spectroscopy (XPS), using a Scienta Omicron spectrometer, model ESCA+, equipped with an EA125 hemispherical analyzer, an XM 1000 monochromator and an X-ray source of Al Kα (1486.7 eV).

2.4. Investigation of catalytic reusability

Esterification reactions of oleic acid with methanol were performed up to the fourth reaction cycle for each catalyst obtained from the different carbonization temperatures, to evaluate catalytic activity and stability. The catalysts were reused after washing with ethanol (99.8%) and n-hexane (95%), vacuum filtration using quantitative filter paper, and drying in an oven at 100 °C for 2 h before each reuse cycle.

The experiments were conducted in a Parr model 5000 Multi-Reactor System, as shown in Fig. 1c. The same reaction conditions was used in the investigation of catalytic reusability for all esterification processes: methanol to oleic acid molar ratio of 20:1, catalyst concentration of 5% (m/m), temperature and reaction time of 90 °C and 1.5 h, respectively. The reaction conditions were determined from literature data collection and preliminary tests (Lathiya et al., 2018; Corrêa et al., 2020; Sangar et al., 2019). Esterification reactions using only biochars and the reaction system (oleic acid and methanol mixture) without the presence of catalyst (white) were performed under the same reaction conditions described for the investigation of reuse processes, to evidence the catalytic performance of the catalysts.

At the end of the experiments, the reaction mixtures were centrifuged and the catalysts were recovered. Then, the reaction products were transferred to a decanting funnel and washed with distilled water portions heated to 90 °C for removal of water and residual alcohol. After that, the products were dried in an oven at 80 °C for 24 h and stored in vials for further analysis.

The conversion, in the face of esterification reactions, was determined by the evaluation of the acidity indexes between the biodiesel produced and the oleic acid. The acidity index was determined by titrimetric method according to AOCS Cd 3d-63, and the conversion of free fatty acids (FFA) was determined using Eq. (2):

$$FFA \; conversion \; (\%) = \left(1 - \frac{AV_f}{AV_i}\right) \times 100 \qquad (2)$$

where AV_i is the Initial Acidity Index (oleic acid) and AV_f is the Acidity Index of the obtained product, given in mg KOH g^{-1}.

2.5. Influence of reaction conditions on catalyst reuse

The influence of the variables temperature and reaction time on the esterification of oleic acid with methanol was evaluated, regarding catalytic performance and catalyst reuse capacity. Thus, for each catalyst, a complete factorial planning of two levels and two variables was carried out, plus 3 central point reactions to estimate the experimental error of the process. For each reaction conditions of the planning, the catalyst was used and reused, totaling 2 reactions and 2 responses at each point.

As in the first catalytic reusability study described above, the response to catalytic activity was given in terms of conversion of free fatty acids into esters. The independent variables (temperature and time) as well as levels were selected by means of preliminary tests. Table 1 presents the coding of the variables and levels adopted in the experiments.

The responses obtained from the experiments were analyzed by calculating effects and percentage of effects for each variable and its interaction, to verify the investigated variables of greater relevance for the esterification processes. The calculations were made with the aid of the GNU Octave Program version 4.2.1 (John W. Eaton and collaborators©, 2017).

3. Results and discussion

The mass yield of the carbonization of the murumuru kernel shell showed a gradual decrease with the increase in temperature, from 34.30% at 450 °C, to 32.05% at 600 °C, reaching 24.30% at 750 °C. According to Cheng and Li. (2018), the higher the pyrolysis temperature, the more volatile components are released from the surface of the material, resulting in lower yield of the carbonized material.

Table 1 Levels of the variables in the Experimental Design.

Independent Variables	Levels		
	−1 (lower)	0 (central)	+1 (higher)
V_1 – Temperature (°C)	70	95	120
V_2 – Time (h)	0.5	1.75	3

– Reactions conducted at 20:1 Molar Ratio and 5% catalyst concentration.

For the density values of $-SO_3H$, before the sulfonation process, all biochars showed non-significant results, around 0.08 mmol g^{-1} ± 0.010. However, after sulfonation, the density of sulfonic groups increased considerably, evidencing the efficacy of the sulfonation process, which resulted in values similar to those found in the literature for this type of material, about 1.0 mmol g^{-1} (Lathiya et al., 2018; Cao et al., 2021; Zhang et al., 2021). The catalysts synthesized with the highest carbonization temperatures showed higher densities of $-SO_3$-H, 1.70 mmol g^{-1} ± 0.017 for BC600-S and 1.50 mmol g^{-1} ± 0.020 for BC750-S, compared to 1.20 mmol g^{-1} ± 0.023 of BC450-S. The slight reduction observed for the carbonized catalyst at 750 °C can be associated to the fact that carbonization temperatures with very high magnitudes reduce the amount of groups $-SO_3H$ that join the edges of carbon structures, since polycondensed aromatic carbon structures are formed at higher degrees (Clohessy and Kwapinski, 2020).

3.1. Influence of carbonization temperature on structure and composition

Fig. 2 exposes the SEM micrographs of biochars and catalysts. In general, there was a predominance of the typical morphology of lignocellulosic biomass with rough surfaces without ordered structures (Scholz et al., 2018).

The SEM micrographs shown in Fig. 2a–c, referring to biochars BC450, BC600 and BC750, respectively, do not show a change in the morphology for products obtained under the variation of carbonization temperature. When analyzing the SEM micrographs of the catalysts, it is noticed that the sulfonation process caused changes in the morphology of BC600-S catalysts (Fig. 2e) and mainly BC750-S (Fig. 2f), which showed apparent pore increment in their structures, because of the corrosion and oxidation of concentrated sulfuric acid (Chen et al., 2022; Konwar et al., 2019). The increase in the number of pores on the catalyst surface is extremely beneficial, since it favors contact between reagents and active sites in the catalytic process (Zhang et al., 2021).

The EDS analysis show that all biochars have carbon as the main element, a common characteristic resulting from the carbonization process, Fig. 3ac. Also, there was a decrease in the amount of oxygen with the increase in carbonization temperature decreasing from 20.36% ± 0.131 in BC450 to about 8.35% ± 0.130 in BC750. Thus, a relative increase in the amount of carbon with the increase in the carbonization temperature was observed. Such variations can be explained by the release of oxygenated volatile components in the carbonization process. Therefore, the increase in carbonization temperature has a positive correlation with the amount of fixed carbon and a negative correlation with the number of oxygenated species (Zhao et al., 2018).
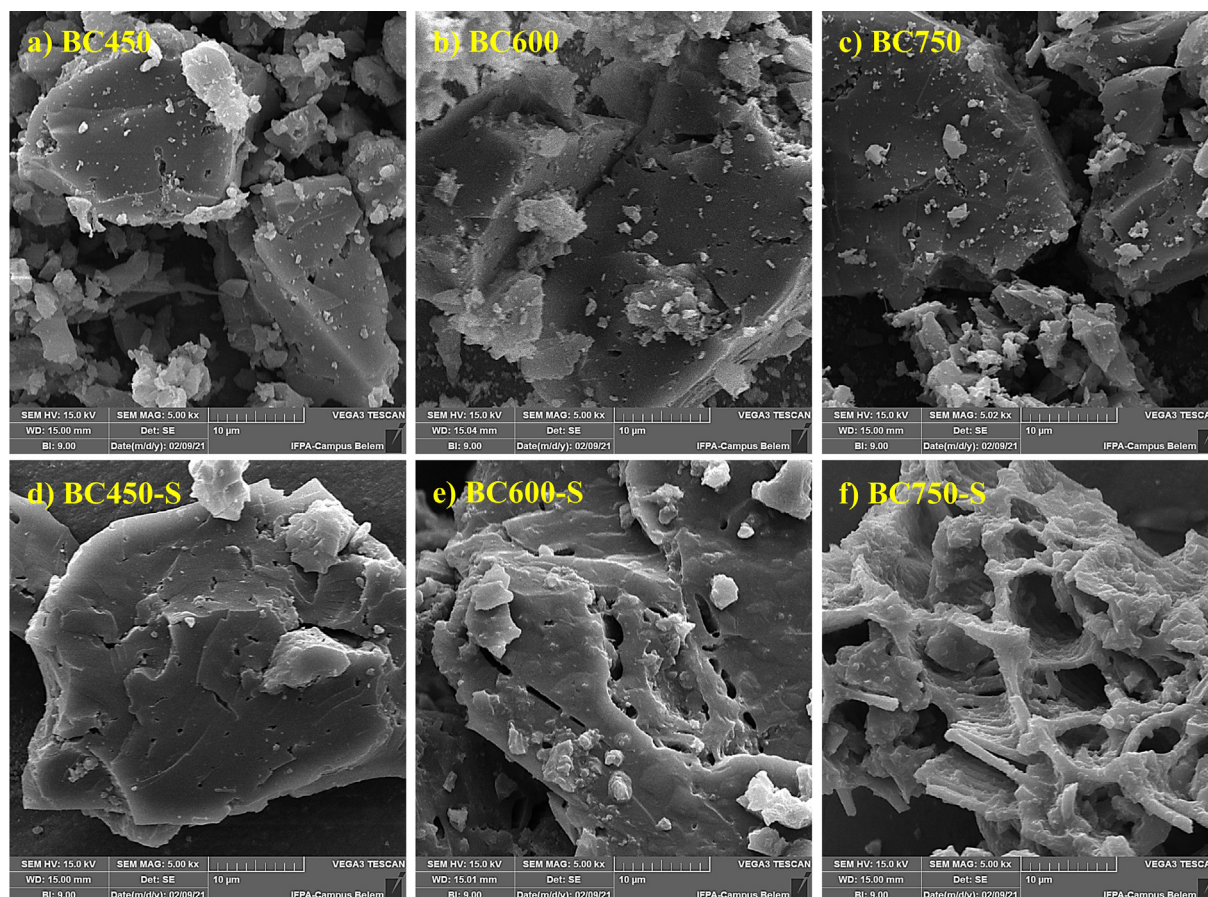

Fig. 2 SEM micrographs, at 5.00 kx magnification, for the biochars in (a), (b) and (c), and their respective catalysts in (d), (e) and (f).
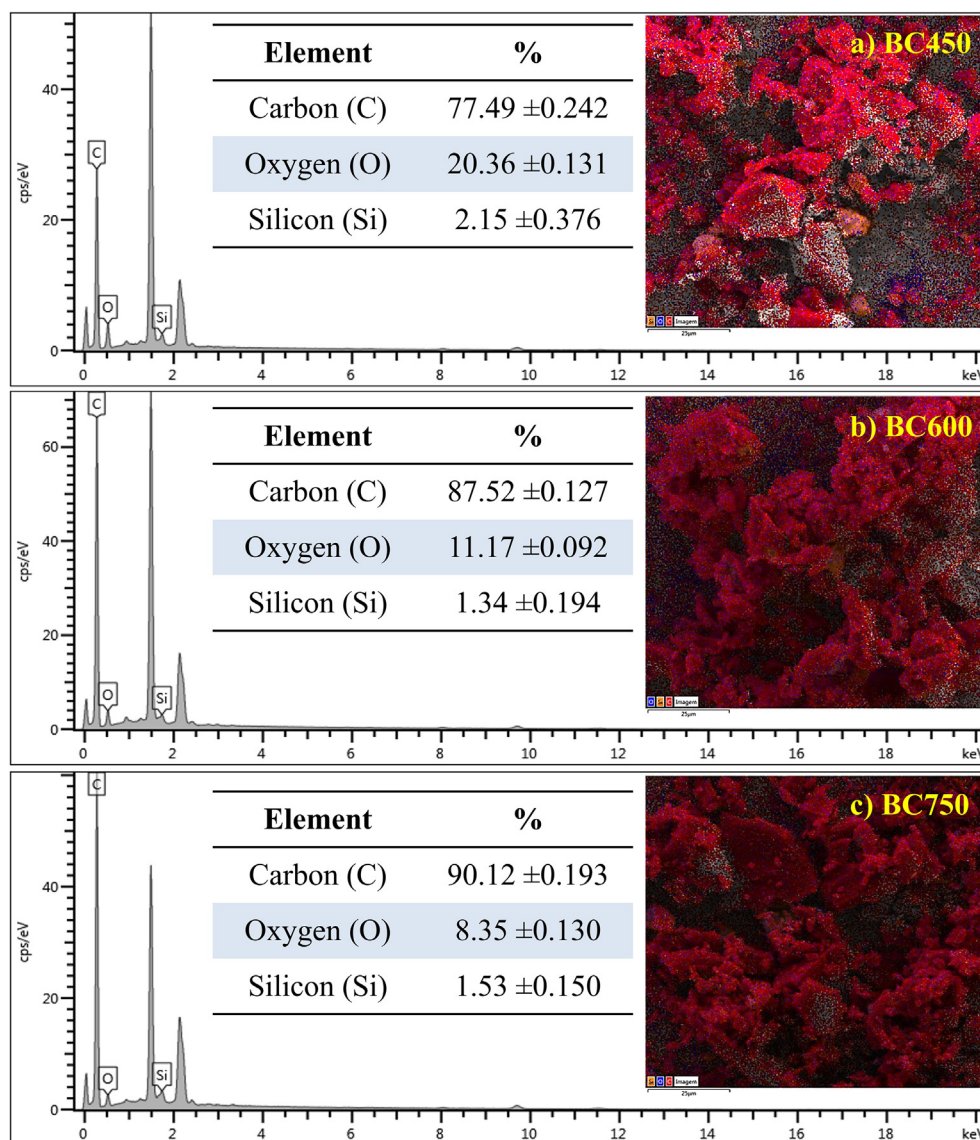
Element	%
Carbon (C)	77.49 ±0.242
Oxygen (O)	20.36 ±0.131
Silicon (Si)	2.15 ±0.376

a) BC450

Element	%
Carbon (C)	87.52 ±0.127
Oxygen (O)	11.17 ±0.092
Silicon (Si)	1.34 ±0.194

b) BC600

Element	%
Carbon (C)	90.12 ±0.193
Oxygen (O)	8.35 ±0.130
Silicon (Si)	1.53 ±0.150

c) BC750

Fig. 3   EDS analysis for biochars: (a) BC450, (b) BC600 and (c) BC750.

The EDS analyses for the catalysts, Fig. 4a–c, verify that carbon is the major element in carbonized materials after sulfonation. However, the percentage increase in oxygen in all materials is noted, suggesting that the sulfonation process favors the formation of oxygenated groups, given that concentrated sulfuric acid used in functionalization is a powerful oxidizing agent. The presence of the sulfur element shows that the process of sulfur groups insertion was efficient, with a lower content (2.55% ± 0.205) for BC450-S (Fig. 4a), and higher content for those with higher carbonization temperatures (8.70% ± 0.187) for BC600-S (Fig. 4b) and (8.37% ± 0.192) BC750-S (Fig. 4c).

Table 2 presents the elemental analysis for biochars, their respective catalysts and catalysts resulting from reuse after the fourth reaction cycle. The catalysts after reuse are marked with the letter R after the corresponding catalyst nomenclature: BC450-S-R, BC600-S-R and BC750-S-R.

According to the EDS analysis, there was an increase of oxygen for sulfonated catalysts in relation to biochars, in addition to the presence of sulfur, which reinforces the effectiveness of the sulfonation process in all carbonized materials. The amount of sulfur increased with the increase of the catalysts carbonization temperature, from about 3.34% (BC450-S) to 6.82% (BC750-S).

According to Sangar et al. (2019), the sulfur and oxygen content increases due to the introduction of the group $-SO_3H$ and formation of $-COOH$ after the sulfonation process. Thus, it was verified that the increase in carbonization temperature favored the functionalization of the material with sulfonic groups.

It is also observed that the H/C ratio decreases with the increase in the carbonization temperature for all materials. The variation of the O/C ratio is best observed for biochars before and after sulfonation, in which there is an increase in the O/C ratio of catalysts in relation to their carbonaceous precursors. A lower H/C ratio represents a decrease in the aliphatic nature, while a high O/C ratio reinforces the increase in oxygenated groups (Oasmaa et al., 2010). Thus, with the
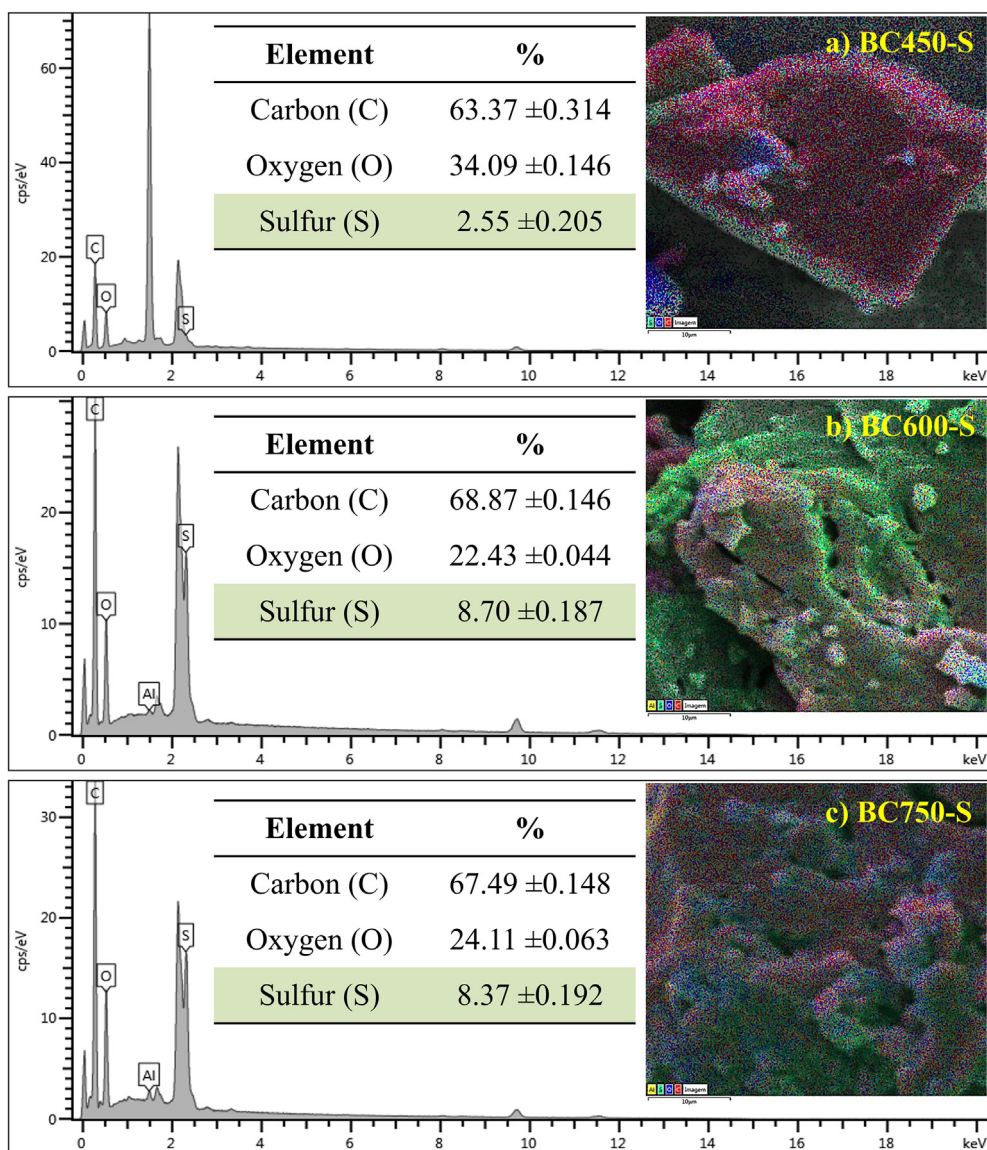
Fig. 4 EDS analysis for the catalysts: (a) BC450-S, (b) BC600-S and (c) BC750-S.

Table 2 Elemental analysis for biochars, their respective catalysts and catalysts after the fourth reaction cycle.

Sample	Elemental composition (%)					Elemental ratio	
	C	H	N	S	O*	H/C	O/C
BC450	76.91 ± 0.040	3.11 ± 0.017	1.67 ± 0.020	<0.03	18.31	0.040	0.24
BC600	88.38 ± 0.034	2.49 ± 0.014	2.97 ± 0.011	<0.03	6.16	0.028	0.070
BC750	85.54 ± 0.060	1.54 ± 0.029	< 0.20	<0.03	12.92	0.018	0.15
BC450-S	54.15 ± 0.066	3.24 ± 0.260	3.57 ± 0.023	3.34 ± 0.011	35.70	0.059	0.66
BC600-S	66.75 ± 0.057	2.18 ± 0.014	2.16 ± 0.029	4.52 ± 0.017	24.39	0.033	0.37
BC750-S	65.50 ± 0.08	1.98 ± 0.032	2.62 ± 0.009	6.82 ± 0.026	23.08	0.030	0.35
BC450-S-R	60.07 ± 0.069	2.82 ± 0.020	2.28 ± 0.031	2.05 ± 0.024	32.78	0.047	0.55
BC600-S-R	70.15 ± 0.037	2.34 ± 0.015	2.17 ± 0.013	4.39 ± 0.023	20.95	0.033	0.29
BC750-S-R	72.14 ± 0.065	2.25 ± 0.030	< 0.20	6.12 ± 0.013	19.49	0.031	0.27

* Determined by difference.

increase in carbonization temperature, it is perceived the decrease in the aliphatic nature of the biochar, suggesting that the material carbonized at 750 °C as the one with the most polycondensed nature. In addition, the individual analysis of the O/C ratio shows that the material carbonized at 450 °C as the most oxygenated, both before and after sulfonation.

Based on the main basis for functionalization the magnitude of the sulfur content, it was verified that after the fourth reaction cycle the catalysts BC600-S and BC750-S were able to maintain most of their sulfonic groups, while the BC450-S catalyst presented a significant leaching content of the active species in relation to the others, with a drop of 3.34% before the reaction cycles to 2.05% after reuse. Therefore, when submitted to the same reaction conditions, the BC750-S catalyst is the one that maintains the highest content of sulfonic groups, since it is the material with the highest functionalization.

The ATR-FTIR spectra of biochars and catalysts are illustrated in Fig. 5. It is observed that both in the spectra referring to biochars (Fig. 5a) and in the spectra recorded for the catalysts (Fig. 5b), characteristic bands of components generated in the carbonization of lignocellulosic biomass are identified, such as at 1593 cm^{-1} referring to the normal vibrational mode (NVM) of the stretch associated with the C=C bond of aromatic rings, and at 1704 cm^{-1} attributed to the MNV of the stretch referring to the C=O bond of carboxylic groups (Zhang et al., 2021). However, in Fig. 5b, the absorption band relative to C=O is barely noticeable for catalysts BC600-S and BC750-S, suggesting BC450-S as more abundant in carboxylic groups, since it is the most oxygenated and oxidation-prone material, according to the elementary analysis.

The decrease in band intensity associated with the MNV of the C=C bond in BC600 and BC750, also observed in their respective catalysts, BC600-S and BC750-S (Fig. 5b), suggests a higher degree of graphitization for these materials, as reported by Scholz et al. (2018), which explain that materials carbonized at high temperatures are composed of wide and extensive polyaromatic layers of carbon, where the C=C vibration in ATR-FTIR is not active.

The presence of bands at 1040 cm^{-1} and 1168 cm^{-1}, typical of normal vibration modes associated with symmetrical and asymmetric stretches of the O=S=O bonds of the sulfonic groups is evident for BC450-S and BC600-S catalysts (Scholz et al., 2018; Zhang et al., 2021). However, for BC750-S the band is practically not observed, despite the high sulfur content shown by elemental analysis. This occurred similarly for Scholz et al. (2018), in studies about sulfonated biochars from carbonizations performed at high temperatures, the authors reported that this fact is due to the strong infrared absorption of carbon structures with a high degree of graphitization.

In order to complement investigations into the carbonaceous structure of materials, the Fig. 6 illustrates the Raman spectra of biochar and catalysts. All materials have characteristic bands of carbon material, located at 1350 cm^{-1} (band D – Defect) and 1590 cm^{-1} (G – Graphite). For biochars, regardless the degree of graphitization, the D-band could be assigned to the most active structures, while the G-band may refer to the most stable structures (Scholz et al., 2018; Xu et al., 2018).

The properties relative to the intensity of the bands can be evaluated according to the Xu et al. (2020a), from the deconvolution of the Raman spectrum in a Gaussian curve to the band D and a Lorentziana curve for the Band G. The intensity values of bands D (I_D) and G (I_G) are described in Table S1. For biochars, it was observed a considerable decrease in intensity of the bands with the increase in carbonization temperature, about 5 times from BC450 to BC750. Xu et al. (2018) report that for carbonized materials, with the increase in the degree of structural order, the amount of aliphatic components such as C–H, C–O and C=O, and alkyls substituents of aromatic rings, becomes smaller, resulting in the disappearance of smaller bands and sharpness of bands D and G.

By relating the intensity of band D with the intensity of band G for each material, through the I_D/I_G ratio, it was possible to obtain the fundamental information to confirm the changes in Raman spectral parameters and the structure information represented by them (Xu et al., 2020b). The I_D/I_G ratio increased from 0.53 (BC450) to 0.73 (BC750). After sulfona-
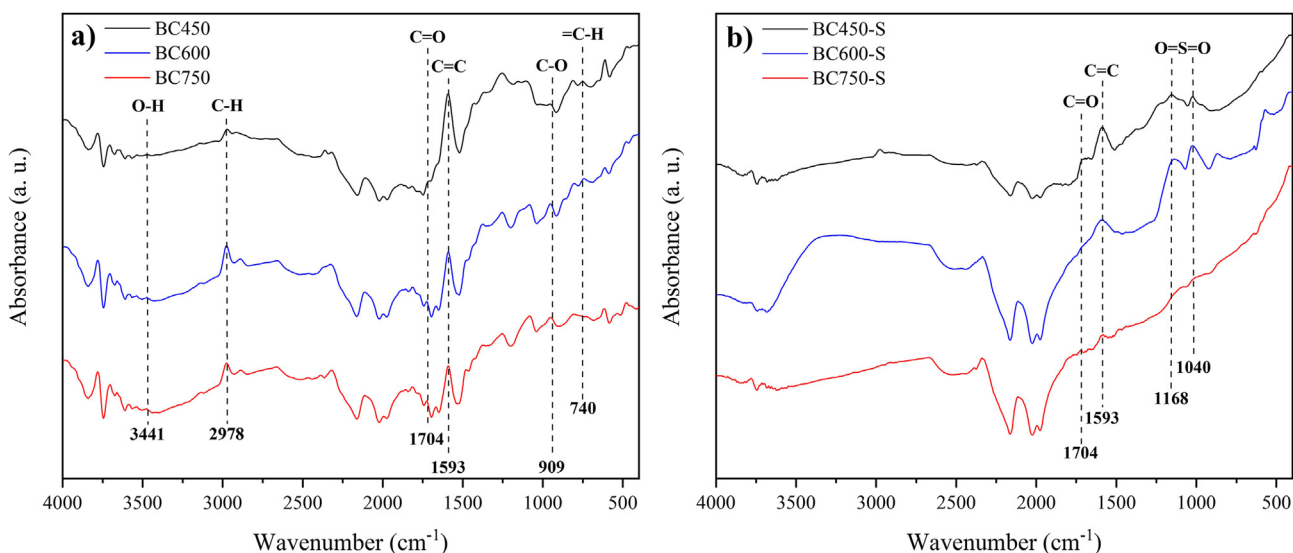

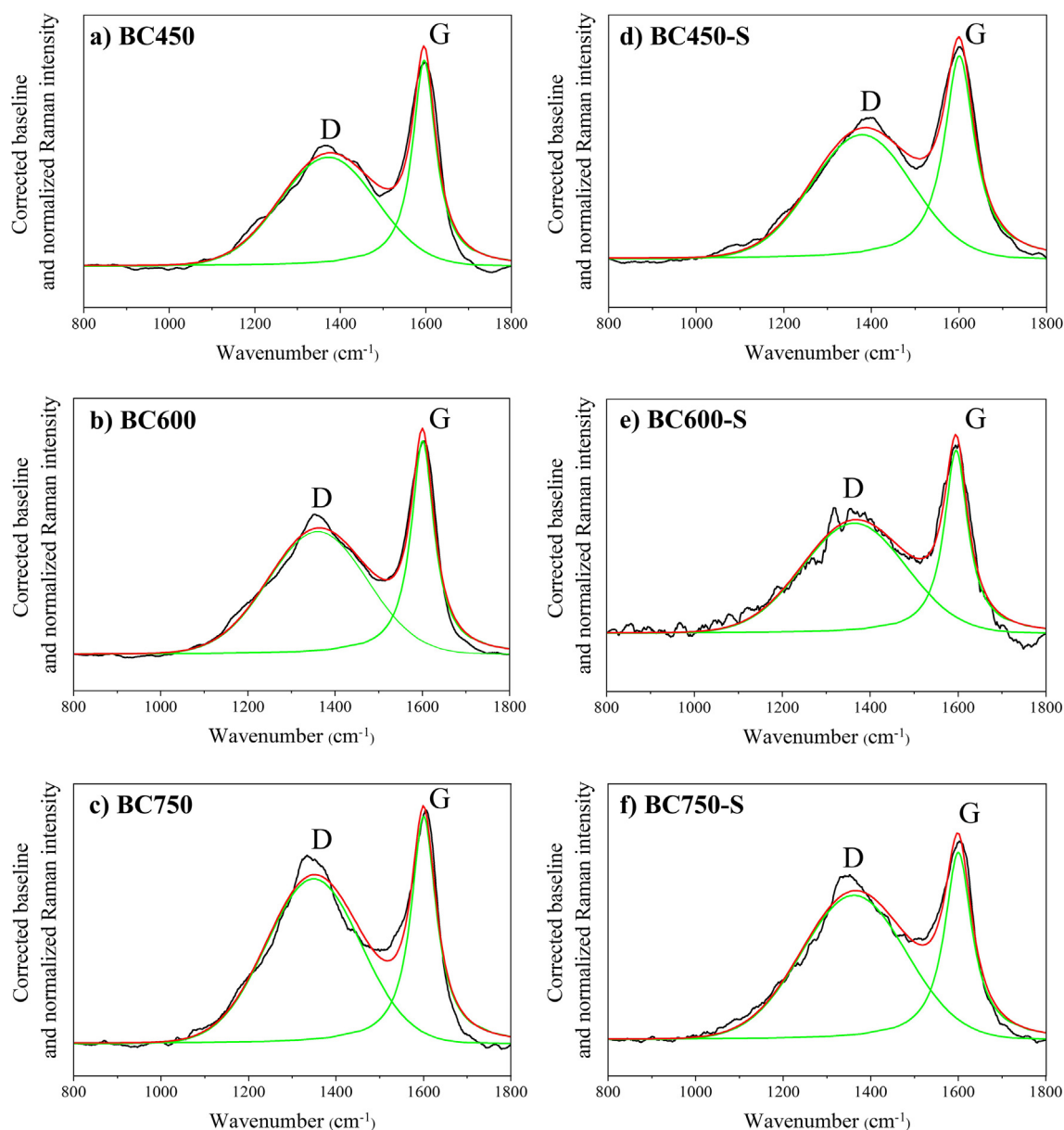**Fig. 5** ATR-FTIR spectrum for materials (a) biochars and (b) catalysts.

Fig. 6 Deconvoluted Raman spectra for the biochars in (a), (b) and (c), and their respective catalysts in (d), (e) and (f).

tion, the BC450-S presented a value of 0.61 (similar to BC600-S), while the BC750-S presented 0.77. The decrease of small aromatic rings and substituting groups are limited, and the growth of polycondensed aromatic rings occurs significantly, resulting in increased I_D/I_G ratio (Xu et al., 2020b). Thus, it can be inferred that the biochar obtained at 750 °C in the present study is the one with the most growth of polycondensed aromatic rings.

Thermogravimetric analysis was used to analyze the thermal decomposition profile and provide data on the composition of the materials. The calculation of the first derivative (DTG) shows maximum mass losses. The TG/DTG curves for biochars and their respective catalysts are presented in Fig. 7.

For biochars, the first main event of mass loss, 100 °C, could be attributed to the evaporation of water adsorbed from moisture (Lathiya et al., 2018). Loss events close to 170 °C

occur due to the decomposition of organic matter residues from components of short chains and low molecular weights (Liu and Liu, 2020).

When analyzing the BC450 (Fig. 7a), a significant loss of 41% was observed in the fourth main event, 468–707 °C, which comprises the decomposition range of the oxygenated functional groups (Rechnia-Goracy et al., 2018). Thus, as evidenced by elemental analysis, BC450 biochar has a higher amount of oxygenated organic matter on the surface than the others, which was previously expected, due to the lower carbonization temperature.

TG/DTG curves for catalysts show that the first mass loss event in the temperature range 25–155 °C, as well as for biochars, is related to water adsorbed on the surface. However, the catalysts showed much higher mass losses than biochars, 19.22% in BC450-S (Fig. 7d) when compared to 3.79% in BC450 (Fig. 7a), a fact that may be associated with the high
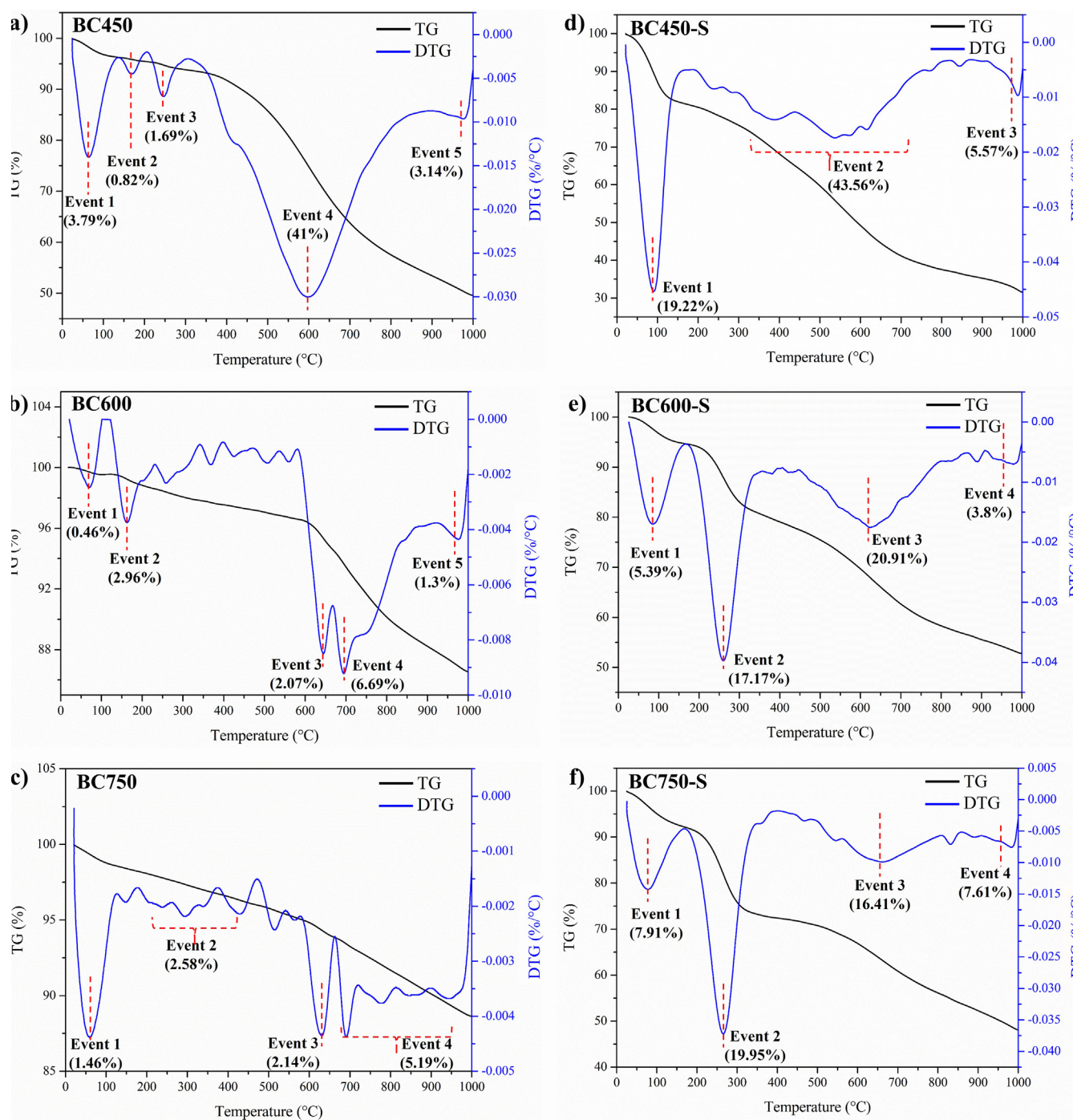
Fig. 7 TG/DTG curves for the biochars in (a), (b) and (c), and their respective catalysts in (d), (e) and (f).

density of polar functional groups, as carboxylic acids and the high hydrophilicity of the sulfonic groups present in catalysts in relation to their carbonaceous precursors (Farabi et al., 2019; Rocha et al., 2019).

The thermal decomposition profile of the BC600-S (Fig. 7e) and BC750-S (Fig. 7f) are very similar. Mass loss events in the temperature range 220–290 °C are interpreted as a result of sulfonic groups decomposition (Corrêa et al., 2020; Chellappan et al., 2018). Thus, the mass loss for the BC750-S catalyst (19.95%) was slightly higher than for BC600-S (17.17%), suggesting a greater number of sulfonic groups in

it, fact corroborated by the evaluation of the sulfur content in the elemental analysis. The third mass loss event, 500–730 °C, corresponds to the decomposition of oxygenated functional groups, as alcoholics/phenolic and carboxylic acids, that may have been introduced because of the sulfonation process (Rechnia-Goracy et al., 2018). Therefore, the mass loss for BC600-S (20.91%) was higher than BC750-S (16.41%), indicating the highest content of oxygenated groups in BC600-S.

The BC450-S catalyst (Fig. 7d) did not present the mass loss events characteristic of the sulfonic groups and well-defined oxygenated groups, although EDS analysis and

elemental analysis showed the presence of sulfur in the material. There was a significant mass loss event of 43.56% in the temperature range of 300–700 °C, in which it is suggested to be responsible for the departure of sulfonic groups and oxygenated groups in the same event, in view of the characteristic ranges already mentioned of 220–290 °C to sulfonic groups decomposition and 500–730 °C to oxygenated groups decomposition.

From the thermogravimetric analysis of the materials, it was observed that all catalysts remain stable in the reaction conditions of catalytic tests employed (temperature range of 70–120 °C). The TG/DTG analyses also reinforce that the increase in carbonization temperature favors functionalization with sulfonic groups, besides corroborating the idea pointed out by the EDS and elementary analyses regarding the negative correlation of the carbonization temperature increase with the amount of oxygenated functional groups.

The TG/DTG analyses for catalysts after the fourth reaction cycle are evidenced in Fig. S1. From TG analysis, it was found that all catalysts showed a small event, designated event 3, corresponding to mass loss between 2% and 3%, associated with the temperature range of 300–400 °C, This is reinforced by the maximum mass loss indicated in DTG analysis. This event may be related to the deposition of impurities and reaction products on the catalyst surface, since such events are not visualized before the use of the catalyst.

From TG/DTG analysis for the BC450-S catalyst (Fig. S1a), a mass loss event (event 2) associated with the decomposition of sulfonic groups is observed in the temperature range of 220–290 °C, with little significant mass loss of about 4.56%. However, a significant mass loss event is noticed between 350 and 700 °C (event 4), of about 37.69%. This fact indicates that despite the leaching of sulfur reported in the elemental analysis and the tendency to decrease oxygenated groups with successive reaction cycles, the catalyst still has a wide variety of functional groups, mainly oxygenated, linked to the carbonaceous structure, even after the fourth reaction cycle (Corrêa et al., 2020; Song et al., 2012).

The thermal decomposition profile for the catalysts BC600-S (Fig. S1b) and BC750-S (Fig. S1c) followed similar to each other, with trends close to that of the catalysts before the reaction cycles. The event associated with the decomposition of sulfonic groups, described as event 2 in the temperature range of 220–290 °C, it showed a slight decrease in both catalysts, mass loss from 17.17% to 10.47% in BC600-S and mass loss from 19.95% to 16.96% in BC750-S, corroborating the small leaching pointed out by elemental analysis and confirming that after the catalytic reactions the BC750-S catalyst maintains sulfonic groups to a greater degree.

To complement the investigation on the process of functionalization of catalysts, XPS were performed for such materials. Fig. 8 illustrates the full-scan XPS spectra, in which it is possible to clearly observe the characteristic bands of this type of catalyst, corresponding to Oxygen 1s, Carbon 1s and Sulfur 2p (Zhang et al., 2021; Estevez et al., 2020).

Fig. 9 details the spectra in the Region of C 1s, O 1s and S 2p for the catalysts. The carbon (C 1s), oxygen (O 1s) and sulfur (S 2p) peaks evidenced in Fig. 7 were deconvoluted in Gaussian curves, similar to that developed by Yu et al. (2021), to explore the functional groups related to the different oxidation states of these elements.
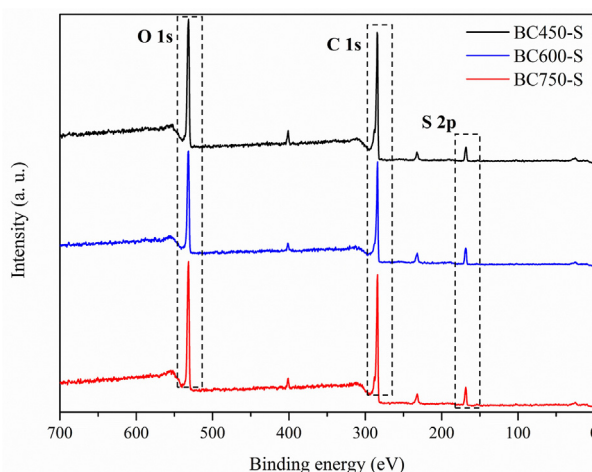

Fig. 8 Full-scan XPS spectra for the catalysts.

In the C 1s spectra of catalysts BC450-S (Fig. 9a), BC600-S (Fig. 9b) and BC750-S (Fig. 9c), the peaks at approximately 284.69 eV are attributed to the C—C/C=C bonds in the aromatic and aliphatic structures, while that at 285.08 and 286.2 eV are related to C—O—C and C—O bonds of alcohol and ether groups, respectively. The peaks around 288.35 eV correspond to C=O/O—C=O in carbonyl and carboxyl groups (Ghosh et al., 2020; Nda-Umar et al., 2020; Yu et al., 2021). The peaks around 288.35 and 285.08 eV are more evident for the BC450-S, which are consistent with the ATR-FTIR and EDS analysis that point this catalyst as the most abundant in carboxylic and more oxygenated surface groups. The peak close to 284 eV is referring to the C—S bond and is considerable in all catalysts. Thus, it is observed that the higher the carbonization temperature of the catalyst, the more highlight the curve of the C—S band gains in relation to the other ones, suggesting that more sulfur groups are being introduced into the carbonaceous structure of the materials (Dong et al.,2018; Yu et al., 2021; Zhong et al., 2019).

For the spectra referring to O 1s of the BC450-S catalysts (Fig. 9d), BC600-S (Fig. 9e) and BC750-S (Fig. 9f), the deconvolution of the spectra at peaks located at 531.16 eV, 532.5 eV, 533 eV and 533.68 eV shows bonds associated with groups O—H, C=O, C—O and O = C—O, respectively (Yu et al., 2021; Yang et al., 2016). The peak attributed to the O—H group stands out in the spectra of all catalysts, mainly BC450-S and BC750-S, probably because the BC450-S is the most oxygenated surface material (EDS and elemental analyses) and the BC750-S is more resistant to the oxidative process of sulfonation in relation to BC600-S, due to its lower aliphatic nature (elemental analysis).

The spectra in the S 2p region for the catalysts BC450-S, BC600-S and BC750-S are exposed in the Fig. 9g–i, respectively. In general, the higher the oxidation state of the sulfur atom, the greater the electron bond energy in the 2p orbitals (Landwehr et al., 2018). The groups can be observed by spectrum deconvolution in three peaks at 169.07 eV, 168.44 eV and 167.76 eV, corresponding to S=O, S—O and S—C, respectively (Yu et al., 2021). The allocation of different sulfur groups to a specific bond energy refers to the dominant $2p_{3/2}$ signal (Landwehr et al., 2018). The peaks of S=O, S—O and
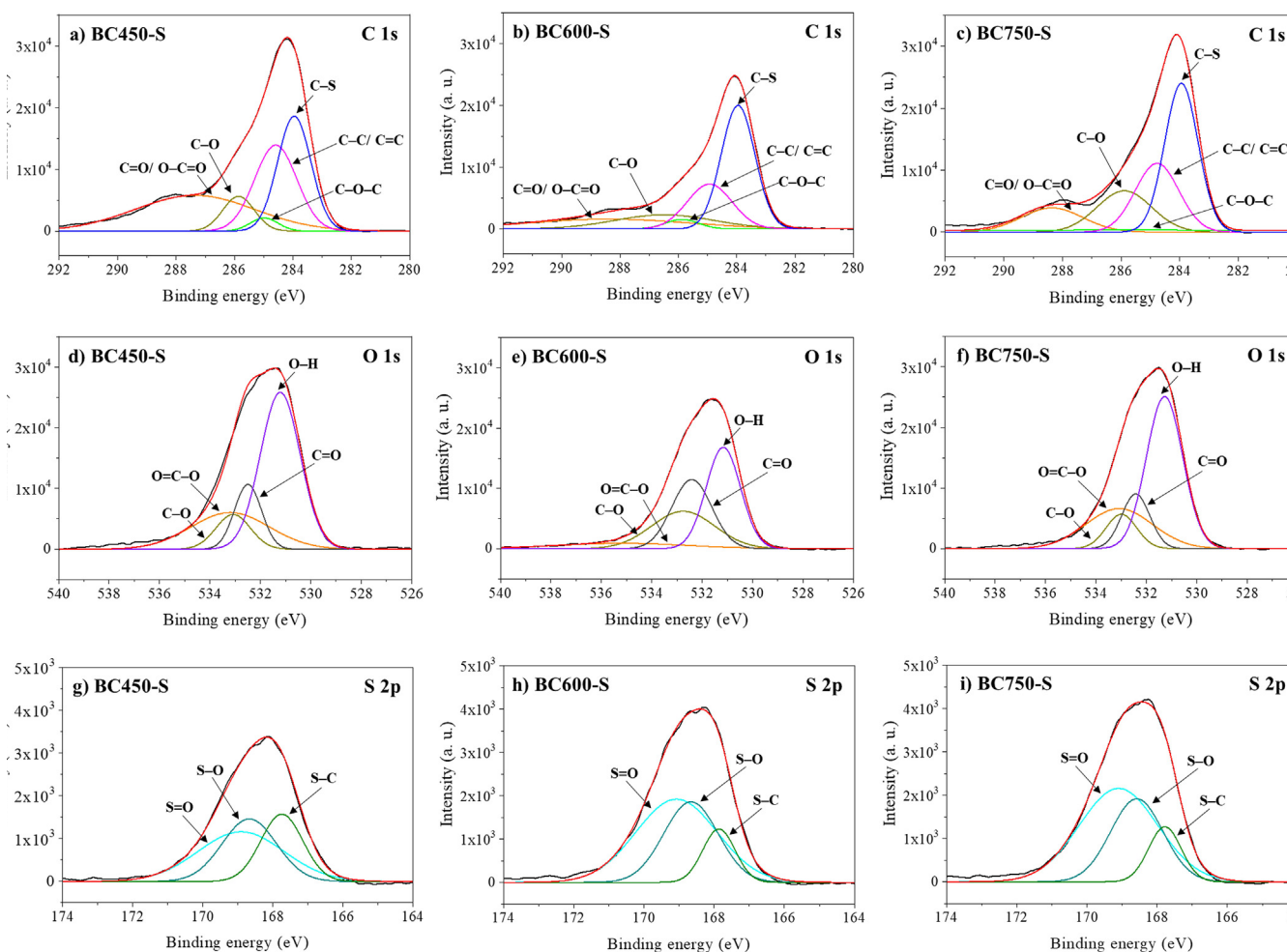
Fig. 9 XPS spectra of C 1s in (a), (b) and (c), O 1s in (d), (e) and (f) and S 2p in (g), (h) and (i), for BC450-S, BC600-S and BC750-S catalysts, respectively.

S—C very evident in the three catalysts confirm that the SO_3H groups were incorporated into the carbonaceous structure of these materials (Yu et al., 2021). Thus, as proposed by Landwehr et al. (2018) in which the sulfonic groups can be inserted in the carbon chain or in the hydroxyl groups, it can be assumed that the functionalization with sulfonic groups occurred mainly directly in the carbon chain of biochars.

According to Konwar et al. (2019), the bond of the sulfonic group can occur in the aliphatic or aromatic structures of the carbon chain. With this, the slight displacement to higher binding energy in the spectra of catalysts BC600-S and BC750-S, which implies an increase in representation of the S=O band, may be related to the predominant bond of the sulfonic groups to the aromatic rings, since their carbonaceous precursors are biochars with more polycondensed and graphitic structures in relation to the BC450-S. Thus, due to the more heterogeneous nature of the BC450-S catalyst and relating to the TG analysis for this material, in which there was no well-defined mass loss event for sulfonic and oxygenated groups, it was assumed that the SO_3H groups are distributed on the surface of this catalyst in large numbers in the aliphatic structures of the carbon chain. Therefore, from the XPS analyses, it is observed that regardless of the degree of graphitization of biochars, the sulfonic groups were efficiently incorporated into the carbona-

ceous structures and may be distributed in aliphatic or aromatic structures depending on the polycondensed structure of the biochar.

3.2. Reusability and stability of the catalyst

The esterification reaction of oleic acid with methanol without the presence of catalyst showed conversion of 6.50%, while the esterification reaction in the presence of non-sulfonated biochars showed conversion of 8.50% for BC450, 7.40% for BC600 and 6.90% for BC750. These results reinforce the effectiveness of the sulfonation process, since the use of biochars without functionalization is not efficient in promoting high conversions of free fatty in biodiesel. The results of the investigation of the catalytic activity and stability of catalysts, based on the reuse process in four successive reaction cycles of oleic acid esterification with methanol, are illustrated in Fig. 10.

The BC450-S catalyst (Fig. 10a) showed a variation in fatty acid conversion from 96.30% ± 1.193 in its first reaction cycle to 45.40% ± 1.011 in the second cycle, which represents a great decrease in catalytic activity in the first reuse process. On the other hand, the BC600-S catalyst (Fig. 10b) presented better catalytic performance when compared to BC450-S.
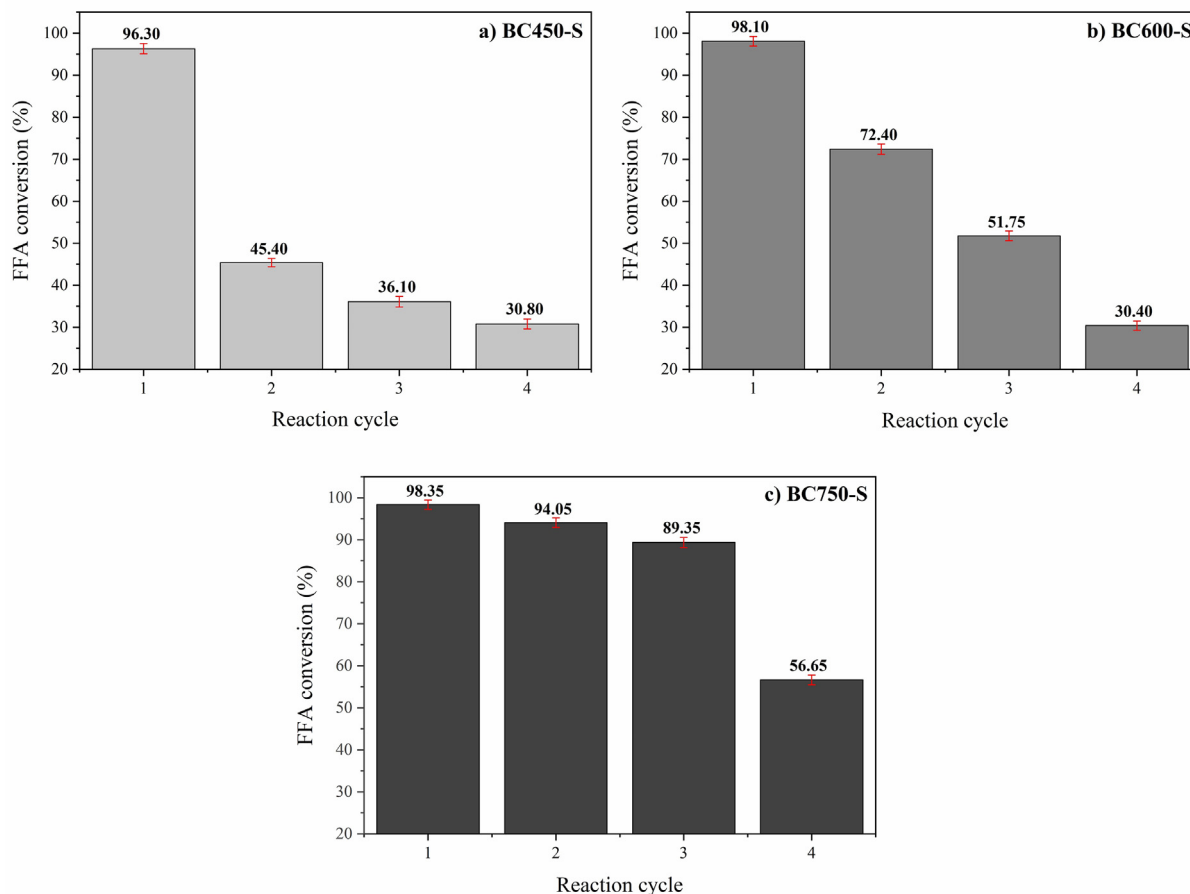
Fig. 10 Reusability and stability of catalysts: (a) BC450-S, (b) BC600-S and (c) BC750-S.

Conversion in the first reaction reached 98.10% ± 1.136 and decreased to 72.40% ± 1.250 in the second reaction cycle. However, it was possible to observe that the BC750-S catalyst (Fig. 10c) maintained high catalytic performance, close to 90%, until the third reaction cycle. Therefore, the BC750-S is characterized as a catalyst of better activity and catalytic stability in the tests employed. Thus, it can be stated that the increase in carbonization temperature results in increased stability of the sulfonated carbon catalyst, probably because a high carbonization temperature can promote stable polycyclic aromatic carbon formation and therefore increase biochar stability (McBeath et al., 2015). According to observed by H/C ratio of elemental analysis and Raman spectroscopy, higher carbonization temperatures lead to biochars with a more poly-condensate nature.

Leaching of the sulfonic groups is reported as one of the main causes of catalytic efficiency reduction of sulfonated biochars (Zhang et al., 2021). The elemental analysis, present in Table 2, revealed that the BC450-S catalyst has greater leaching of the sulfur element after the reuse processes, which consequently will lead to a greater reduction of its catalytic activity when compared to the others. The BC600-S catalyst has not lost a large amount of sulfur, but the BC750-S has a greater amount of sulfonic groups after reuse, which justifies its better catalytic performance even though other factors such as the loss of mass between reaction cycles, or the blocking of active catalyst sites by product residues have contributed to the deactivation of catalysts.

3.3. Influence of temperature and reaction time on catalyst reuse

The results obtained for the use and reuse of catalysts (first and second reaction cycle) from Factorial Planning are shown in Table 3. Experiments 1 through 7 refer to the BC450-S catalyst, while those from 8 to 14 are related to BC600-S, and those from 15 to 21 refer to the BC750-S catalyst.

In general, it is observed that in the first reaction cycle almost all experiments showed high conversions (>80%), except when the two variables (Temperature and Time) are at low levels. In the second reaction cycle for the BC450-S catalyst, only experiment 4, when the two variables are at a high level, showed high conversion (~93%). For the BC600-S catalyst, in the second reaction cycle, experiments 9 and 11 obtained conversions close to 90%, reinforcing the greater reuse capacity of the BC600-S catalyst in relation to the BC450-S. While the BC750-S catalyst showed most reactions with high conversions (>80%), in which the decrease in conversion rates occurred only when the temperature variable is at a low level.

According to the investigation of reusability and catalytic stability discussed above, the BC450-S catalyst showed a great

Table 3 Experimental matrix and conversion results obtained for the first and second reaction cycles of the catalysts.

Catalyst	Exp.	Variables		Response (Conversion – %)	
		Temperature (°C) V_1	Time (h) V_2	1° Cycle (R_1)	2° Cycle (R_2)
BC450-S	1	70 (−1)	0.5 (−1)	48.30	24.80
	2	120 (+1)	0.5 (−1)	97.30	58.85
	3	70 (−1)	3 (+1)	84.20	48.30
	4	120 (+1)	3 (+1)	97.80	93.30
	5	95 (0)	1.75 (0)	97.60	58.20
	6	95 (0)	1.75 (0)	97.10	56.80
	7	95 (0)	1.75 (0)	96.80	53.60
BC600-S	8	70 (−1)	0.5 (−1)	64.60	25.80
	9	120 (+1)	0.5 (−1)	98.30	86.30
	10	70 (−1)	3 (+1)	98.05	48.60
	11	120 (+1)	3 (+1)	98.10	97.60
	12	95 (0)	1.75 (0)	98.30	69.00
	13	95 (0)	1.75 (0)	98.30	66.20
	14	95 (0)	1.75 (0)	98.20	70.20
BC750-S	15	70 (−1)	0.5 (−1)	58.00	17.30
	16	120 (+1)	0.5 (−1)	97.80	80.10
	17	70 (−1)	3 (+1)	97.80	27.10
	18	120 (+1)	3 (+1)	98.10	97.30
	19	95 (0)	1.75 (0)	98.20	85.60
	20	95 (0)	1.75 (0)	97.80	92.80
	21	95 (0)	1.75 (0)	98.00	91.05

decrease in conversion rates in the first reuse process. Thus, from experiment 4, it was possible to observe that the increase in temperature and time in the reaction were able to maintain high conversions in the two consecutive cycles, directly influencing the reuse capacity of this catalyst.

Fig. S2 presents the graph of the Percentage of Effects and graph of the normal probability for the first reaction cycle of the catalysts. In the first reaction cycle of the BC450-S catalyst, temperature was identified as the variable with the greatest influence on the conversion of fatty acids into biodiesel (Fig. S2a). This variable has a positive effect value (Fig. S2b), so the increase in temperature in the investigated interval will provide higher conversions. The variable time and the linear interaction between time and temperature showed similar influences (Fig. S2a), in which the time presents a positive effect value and the interaction between time and temperature has a negative effect value (Fig. S2b). In general, temperature considerably influences the conversion rates of free fatty acids, since the increase in temperature in the reaction medium is closely related to factors such as mass transfer between catalyst and reagents and the adverse effects of methanol vaporization (Kefas et al., 2018; Ong et al., 2014). Thus, it can be inferred that the optimal reaction condition for the application of the BC450-S catalyst, in terms of catalytic stability, is the use of 120 °C temperature and 3 h of reaction time, leading to biodiesels with conversions above 93%, either in the first or second use.

Analyzing the data in Table 3 referring to the BC600-S catalyst, the behavior is similar to the trend presented in the performance of the BC450-S catalyst. However, the conversions values, either in the first or second cycle are above 97%, when the reactions are conducted at the higher levels, i.e. at a temperature of 120 °C and reaction time of 3 h. Moreover, in the first reaction cycle in all experiments using the BC750-S catalyst, biodiesel conversions above 97% are achieved, except

for the experiment using the lower levels, represented in experiment 15. However, when considering the reactions of the second reaction cycle, only the experiments at the central point and the experiment at the upper levels, show some maintenance of catalytic activity to the BC750-S catalyst, making the optimal reaction condition for this catalyst is at a temperature of 90 °C and reaction time of 1.5 h, since under these conditions the catalyst can maintain conversions above 90%. Moreover, this condition represents a relatively lower cost for the use of the catalyst in biodiesel synthesis, when compared with the reaction condition using the temperature of 120 °C and reaction time of 3 h, which also presents in this study high conversion in esters.

For the catalysts BC600-S and BC750-S, in the first reaction cycle the effects of temperature and time, as well as their linear interaction, were similar to each other, each accounting for approximately 33% (Fig. S2c and e) of fatty acid conversion rates. This fact could be attributed to strictly similar values (~97%) of conversions in reaction process.

The effect results obtained for the variables temperature and time in the second reaction cycle of catalysts are exposed in Fig. S3. For the BC450-S catalyst, as in the first reaction cycle, the influence of the temperature variable is notorious and accounts for about 60% of the effects on conversion rates. The effect of the variable time starts to have greater influence in the second cycle in relation to the first cycle (from 20% to 35%), with a positive effect value, while the linear interaction between time and temperature was insignificant. In the second reaction cycle of the BC600-S and BC750-S catalysts, temperature stood out significantly as the factor with the greatest influence on reaction cycles (Fig. S3c and e). The effect of the variable time and the linear interaction between time and temperature can be considered as not significant and insignificant, respectively, within the limits investigated (Fig. S3d and f).

Table 4 Operational conditions in the synthesis of biodiesel and biomass used in the preparation of the sulfonated biochar catalyst.

Biomass	Acid used in sulfonation	Reaction conditions				FFA (%)	FFA (%) in the third cycle	Reference
		T (°C)	Molar ratio	Catalyst concentration (%)	t (h)			
Bamboo powder	H_2SO_4	65	8:1	10	8	98.0	84.7	Zhang et al., 2021
Corncob	H_2SO_4	70	15:1	3	2	92.0	70.0	Ibrahim et al., 2020
Bioasphalt	H_2SO_4	220	16.8:1	0.2	4.5	95.0	N.R	Shu et al., 2010
Oil palm empty fruit bunch	4-BDS	110	30:1	20	7	98.1	N.R	Lim et al., 2020
Bamboo	$C_6H_7NO_3S$	85	7:1	12	3	96.0	~52.0	Niu et al., 2018
Orange peel	H_2SO_4	65	20:1	5	4.5	91.7	38.1	Lathiya et al., 2018
Rice Husk	H_2SO_4	110	20:1	5	15	> 98.0	~85.0	Li et al., 2014
Sargassum horneri	H_2SO_4	70	15:1	10	3	96.4	68.7	Cao et al., 2021
Murumuru kernel shell	H_2SO_4	90	20:1	5	1.5	98.4	89.4	This study

N.R = Not reported; BDS = Benzenediazonium sulfonate.

Since in the second reaction cycle there is less availability of active catalyst sites in relation to the first reaction cycle, the effects of reaction variables gain greater prominence in fatty acid conversions. Thus, for the BC450-S catalyst, considered as less stable in relation to the others (BC600-S and BC750-S), its reuse process can be adapted by varying the reaction conditions, increasing time and temperature, in order to maintain its high catalytic efficiency, without ruling out the possibility of reuse of the catalyst in question. Thus, it is possible to adjust the reaction variables to improve conversion rates in catalytic reuse processes, to use the maximum reuse capacity of each catalyst within the limits of viable reaction parameters. As recommended by the literature, temperature is a factor that considerably influences the esterification reaction (Corrêa et al., 2020; Kefas et al., 2018; Oliveira et al., 2021), since, depending on the other reaction variables, the process requires a certain temperature to provide the activation energy needed to protonate the carbonyl groups of fatty acid to achieve maximum conversion rates (Lokman et al., 2015).

3.4. Comparison of the catalytic activity of solid sulfonated carbon-based catalysts

Table 4 shows the comparison of the biochar catalyst produced in this study with other solid sulfonated carbon-based catalysts reported in literature applied to esterification reaction in biodiesel production. Through the analysis of Table 4, it is noticed that in the present study the catalyst BC750-S obtained a biodiesel with high conversion in less severe reaction conditions, as well as high catalytic stability throughout the three reaction cycles, when compared with other studies, a fact that corroborate the high potential of using the residual biomass of murumuru kernel shell in the development of a new material applied in the biodiesel production.

4. Conclusion

The properties of the sulfonated carbon catalyst, such as structure, activity and catalytic stability, are greatly influenced by the carbonization temperature of biomass. The catalyst from carbonization at 750 °C presented the best catalytic performance and the highest stability, with free fatty acids conversion of 98.35% ± 1.105 in the first reaction cycle and maintenance of this conversion at 89.35% ± 1.197 in the third reaction cycle when employed in the optimal reaction condition: reaction temperature of 90 °C, methanol to oleic acid molar ratio

of 20:1, catalyst concentration of 5% and reaction time of 1.5 h. Thus, for direct pyrolysis processes, high carbonization temperatures trend to promote more polycondensed biochars with greater catalytic activity and stability. The increase of the variable time and especially the reaction temperature can promote reuse processes with high conversion rates to make the most of the capacity of each catalyst with different stabilities. Thus, the present study contributes greatly to the synthesis of new heterogeneous carbon-based acid catalysts applied in the biodiesel production process, since it evidences the impact of carbonization temperature on the insertion of sulfonic groups and their direct correlation with obtaining more active and stable catalysts applied in the esterification reaction. In addition, it reintegrates waste generated in large quantities by the agroindustry into the chain of production processes.

CRediT authorship contribution statement

Ana Paula da Luz Corrêa: Conceptualization, Methodology, Investigation, Visualization, Formal analysis, Writing – original draft. **Paula Maria Melo da Silva:** Methodology, Resources, Investigation. **Matheus Arrais Gonçalves:** Methodology, Resources, Investigation. **Rafael Roberto Cardoso Bastos:** Methodology, Investigation. **Geraldo Narciso da Rocha Filho:** Supervision. **Leyvison Rafael Vieira da Conceição:** Project administration, Conceptualization, Visualization, Supervision, Project administration, Writing – review & editing.

Declaration of Competing Interest

The authors declare that they have no known competing financial interests or personal relationships that could have appeared to influence the work reported in this paper.

Appendix A. Supplementary material

Supplementary material to this article can be found online at https://doi.org/10.1016/j.arabjc.2023.104964.

References

Acharya, R.N., Perez-Pena, R., 2020. Role of comparative advantage in biofuel policy adoption in Latin America. Sustainability 12, 1411–1424. https://doi.org/10.3390/su12041411.

Bastos, R.R.C., Corrêa, A.P.L., Luz, P.T.S., Rocha Filho, G.N., Zamian, J.R., Conceição, L.R.V., 2020. Optimization of biodiesel production using sulfonated carbon-based catalyst from an amazon agro-industrial waste. Energy Convers. Manag. 205,. https://doi.org/10.1016/j.enconman.2019.112457 112457.

Battisti, R., Hafemann, E., Claumann, C.A., Machado, R.A.F., Marangoni, C., 2018. Synthesis and characterization of cellulose acetate from royal palm tree agroindustrial waste. Polym. Eng. Sci. 59 (5), 891–898. https://doi.org/10.1002/pen.25034.

Boumaaza, M., Belaadi, A., Bourchak, M., Juhany, K.A., Jawaid, M., Marvila, M.T., Azevedo, A.R.G., 2023. Optimization of flexural properties and thermal conductivity of Washingtonia plant biomass waste biochar reinforced bio-mortar. J. Mater. Res. And Technol. 23, 3515–3536. https://doi.org/10.1016/j.jmrt.2023.02.009.

Cao, M., Peng, L., Xie, Q., Xing, K., Lu, M., Ji, J., 2021. Sulfonated *Sargassum horneri* carbon as solid acid catalyst to produce biodiesel via esterification. Bioresour. Technol. 324,. https://doi.org/10.1016/j.biortech.2020.124614 124614.

Chellappan, S., Nair, V., Sajith, V., Aparna, K., 2018. Experimental validation of biochar based green bronsted acid catalysts for simultaneous esterification and transesterification in biodiesel production. Bioresour. Technol. 2, 38–44. https://doi.org/10.1016/j.biteb.2018.04.002.

Chellappan, S., Aparna, K., Chingakham, C., Sajith, V., Nair, V., 2019. Microwave assisted biodiesel production using a novel brønsted acid catalyst based on nanomagnetic biocomposite. Fuel 246, 268–276. https://doi.org/10.1016/j.fuel.2019.02.104.

Chen, G., Wang, X., Jiang, Y., Mu, X., Liu, H., 2019. Insights into deactivation mechanism of sulfonated carbonaceous solid acids probed by cellulose hydrolysis. Catal. Today 319, 25–30. https://doi.org/10.1016/j.cattod.2018.03.069.

Chen, X., Zhang, Z., Yuan, B., Yu, F., Xie, C., Yu, S., 2022. Lignin-based sulfonated carbon as an efficient biomass catalyst for clean benzylation of benzene ring compounds. J. Ind. Eng. Chem. 111, 369–379. https://doi.org/10.1016/j.jiec.2022.04.019.

Cheng, F., Li, X., 2018. Preparation and application of biochar-based catalysts for biofuel production. Catalysts 8 (9), 346. https://doi.org/10.3390/catal8090346.

Clohessy, J., Kwapinski, W., 2020. Carbon-based catalysts for biodiesel production – A review. Appl. Sci. 10, 918. https://doi.org/10.3390/app10030918.

Corrêa, A.P.L., Bastos, R.R.C., Rocha Filho, G.N., Zamian, J.R., Conceição, L.R.V., 2020. Preparation of sulfonated carbon-based catalysts from murumuru kernel shell and their performance in the esterification reaction. RSC Adv. 10 (34), 20245–20256. https://doi.org/10.1039/D0RA03217D.

Dechakhumwat, S., Hongmanorom, P., Thunyaratchatanon, C., Smith, S.M., Boonyuen, S., Luengnaruemitchai, A., 2020. Catalytic activity of heterogeneous acid catalysts derived from corncob in the esterification of oleic acid with methanol. Renew. Energy 148, 897–906. https://doi.org/10.1016/j.renene.2019.10.174.

Deris, N.H., Rashid, U., Soltani, S., Choong, T.S.Y., Nehdi, I.A., 2020. Study the effect of various sulfonation methods on catalytic activity of carbohydrate-derived catalysts for ester production. Catalysts 10, 638. https://doi.org/10.3390/catal10060638.

Dhawane, S.H., Kumar, T., Halder, G., 2018. Recent advancement and prospective of heterogeneous carbonaceous catalysts in chemical and enzymatic transformation of biodiesel. Energy Convers. Manag. 167, 176–202. https://doi.org/10.1016/j.enconman.2018.04.073.

Dong, K., Zhang, J., Luo, W., Su, L., Huang, Z., 2018. Catalytic conversion of carbohydrates into 5-hydroxymethyl furfural over sulfonated hyper-cross-linked polymer in DMSO. Chem. Eng. J. 334, 1055–1064. https://doi.org/10.1016/j.cej.2017.10.092.

Estevez, R., Aguado-Deblas, L., Montes, V., Caballero, A., Bautista, F.M., 2020. Sulfonated carbons from olive stones as catalysts in the microwave-assisted etherification of glycerol with tert-butyl alcohol. Mol. Catal. 488,. https://doi.org/10.1016/j.mcat.2020.110921 110921.

Farabi, M.S.A., Ibrahim, M.L., Rashid, U., Taufiq-Yap, Y.H., 2019. Esterification of palm fatty acid distillate using sulfonated carbon-based catalyst derived from palm kernel shell and bamboo. Energy Convers. Manag. 181, 562–570. https://doi.org/10.1016/j.enconman.2018.12.033.

Fraile, J.M., García-Bordejé, E., Pires, E., Roldán, L., 2015. Catalytic performance and deactivation of sulfonated hydrothermal carbon in the esterification of fatty acids: comparison with sulfonic solids of different nature. J. Catal. 324, 107–118. https://doi.org/10.1016/j.jcat.2014.12.032.

Gardy, J., Hassanpour, A., Lai, X., Ahmed, M.H., Rehan, M., 2017. Biodiesel production from used cooking oil using a novel surface functionalised TiO_2 nano-catalyst. App. Catal. B 7, 297–310. https://doi.org/10.1016/j.apcatb.2017.01.080.

Ghodake, G.S., Shinde, S.K., Kadam, A.A., Saratale, R.G., Saratale, G.D., Kumar, M., Palem, R.R., Al-Shwaiman, H.A., Elgorban, A.M., Syed, A., Kim, D., 2021. Review on biomass feedstocks, pyrolysis mechanism and physicochemical properties of biochar: State-of-the-art framework to speed up vision of circular bioeconomy. J. Clean. Prod. 297,. https://doi.org/10.1016/j.jclepro.2021.126645 126645.

Ghosh, A., Singha, A., Auroux, A., Das, A., Sen, D., Chowdhury, B., 2020. A green approach for the preparation of a surfactant embedded sulfonated carbon catalyst towards glycerol acetalization reactions. Catal. Sci. Technol. 10, 4827–4844. https://doi.org/10.1039/d0cy00336k.

Gonçalves, M.A., Mares, E.K.L., Zamian, J.R., Rocha Filho, G.N., Conceição, L.R.V., 2021. Statistical optimization of biodiesel production from waste cooking oil using magnetic acid heterogeneous catalyst $MoO_3/SrFe_2O_4$. Fuel 304,. https://doi.org/10.1016/j.fuel.2021.121463 121463.

Ibrahim, S.F., Asikin-Mijan, N., Ibrahim, M.L., Abdulkareem-Alsultan, G., Izham, S.M., Taufiq-Yap, Y., 2020. Sulfonated functionalization of carbon derived corncob residue via hydrothermal synthesis route for esterification of palm fatty acid distillate. Energy Convers. Manag. 210,. https://doi.org/10.1016/j.enconman.2020.112698 112698.

Kefas, H.M., Yunus, R., Rashid, U., Taufiq-Yap, Y.H., 2018. Modified sulfonation method for converting carbonized glucose into solid acid catalyst for the esterification of palm fatty acid distillate. Fuel 229, 68–78. https://doi.org/10.1016/j.fuel.2018.05.014.

Konwar, L.J., Mäki-Arvela, P., Mikkola, J., 2019. SO₃H–containing functional carbon materials: synthesis, structure, and acid catalysis. Chem. Rev. 119 (22), 11576–11630. https://doi.org/10.1021/acs.chemrev.9b00199.

Landwehr, J., Steldinger, H., Etzold, B.J.M., 2018. Introducing sulphur surface groups in microporous carbons: a mechanistic study on carbide derived carbons. Catal. Today 301, 191–195. https://doi.org/10.1016/j.cattod.2017.05.027.

Lathiya, D.R., Bhatt, D.V., Maheria, K.C., 2018. Synthesis of sulfonated carbon catalyst from waste orange peel for cost effective biodiesel production. Bioresour. Technol. Rep. 2, 69–76. https://doi.org/10.1016/j.biteb.2018.04.007.

Li, M., Zheng, Y., Chen, Y., Zhu, X., 2014. Biodiesel production from waste cooking oil using a heterogeneous catalyst from pyrolyzed rice husk. Bioresour. Technol. 154, 345–348. https://doi.org/10.1016/j.biortech.2013.12.070.

Lim, S., Yap, Y., Pang, Y.L., Wong, K.H., 2020. Biodiesel synthesis from oil palm empty fruit bunch biochar derived heterogeneous solid catalyst using 4-benzenediazonium sulfonate. J. Hazard. Mater. 390,. https://doi.org/10.1016/j.jhazmat.2019.121532 121532.

Liu, Z., Liu, Z., 2020. Comparison of hydrochar- and pyrochar-based solid acid catalysts from cornstalk: physiochemical properties, catalytic activity and deactivation behavior. Bioresour. Technol. 297,. https://doi.org/10.1016/j.biortech.2019.122477 122477.

Lokman, I.M., Rashid, U., Taufiq-Yap, Y.H., Yunus, R., 2015. Methyl ester production from palm fatty acid distillate using sulfonated glucose-derived acid catalyst. Renew. Energy 81, 347–354. https://doi.org/10.1016/j.renene.2015.03.045.

Mares, E.K.L., Gonçalves, M.A., Luz, P.T.S., Rocha Filho, G.N., Zamian, J.R., Conceição, L.R.V., 2021. Acai seed ash as a novel basic heterogeneous catalyst for biodiesel synthesis: optimization of the biodiesel production process. Fuel 299,. https://doi.org/10.1016/j.fuel.2021.120887 120887.

Mcbeath, A.V., Wurster, C.M., Bird, M.I., 2015. Influence of feedstock properties and pyrolysis conditions on biochar carbon stability as determined by hydrogen pyrolysis. Biomass Bioenergy 73, 155–173. https://doi.org/10.1016/j.biombioe.2014.12.022.

Nda-Umar, U.I., Ramli, I., Muhamad, E.N., Azri, N., Taufiq-Yap, Y.H., 2020. Optimization and Characterization of Mesoporous Sulfonated Carbon Catalyst and Its Application in Modeling and Optimization of Acetin Production. Molecules 25, 5221. https://doi.org/10.3390/molecules25225221.

Ning, Y., Niu, S., 2017. Preparation and catalytic performance in esterification of a bamboo-based heterogeneous acid catalyst with microwave assistance. Energy Convers. Manag. 153, 446–454. https://doi.org/10.1016/j.enconman.2017.10.025.

Niu, S., Ning, Y., Lu, C., Han, K., Yu, H., Zhou, Y., 2018. Esterification of oleic acid to produce biodiesel catalyzed by sulfonated activated carbon from bamboo. Energy Convers. Manag. 163, 59–65. https://doi.org/10.1016/j.enconman.2018.02.055.

Oasmaa, A., Solantausta, Y., Arpiainen, V., Kuoppala, E., Sipila, K., 2010. Fast pyrolysis bio-oils from wood and agricultural residues. Energy Fuels 24, 1380–1388. https://doi.org/10.1021/ef901107f.

Oliveira, A.N., Ferreira, I.M., Jimenez, D.E.Q., Neves, F.B., Silva, L.S., Costa, A.A.F., Lima, E.T.L., Pires, L.H.O., Costa, C.E.F., Rocha Filho, G.N., Nascimento, L.A.S., 2021. An efficient catalyst prepared from residual kaolin for the esterification of distillate from the deodorization of palm oil. Catalysts 11 (5), 604. https://doi.org/10.3390/catal11050604.

Ong, H.R., Khan, M.R., Chowdhury, M.N.K., Yousuf, A., Cheng, C.K., 2014. Synthesis and characterization of CuO/C catalyst for the esterification of free fatty acid in rubber seed oil. Fuel 120, 195–201. https://doi.org/10.1016/j.fuel.2013.12.015.

Pereira Filho, E.R., 2018. Planejamento fatorial em química: maximizando a obtenção de resultados. Série Apontamentos, São Carlos.

Pesce, C., 2009. Oleaginosas da Amazônia. Museu Paraense Emílio Goeldi, Núcleo de Estudos Agrários e Desenvolvimento Rural, Belém.

Rechnia-Goracy, P., Malaika, A., Kozłowski, M., 2018. Acidic activated carbons as catalysts of biodiesel formation. Diam. Relat. Mater. 87, 124–133. https://doi.org/10.1016/j.diamond.2018.05.015.

Rocha, P.D., Oliveira, L.S., Franca, A.S., 2019. Sulfonated activated carbon from corn cobs as heterogeneous catalysts for biodiesel production using microwave-assisted transesterification. Renew. Energy 143, 1710–1716. https://doi.org/10.1016/j.renene.2019.05.070.

Sangar, S.K., Lan, C.S., Razali, S.M., Farabi, M.A., Taufiq-Yap, Y.H., 2019. Methyl ester production from palm fatty acid distillate (PFAD) using sulfonated cow dung-derived carbon-based solid acid catalyst. Energy Convers. Manag. 196, 1306–1315. https://doi.org/10.1016/j.enconman.2019.06.073.

Schalchli, H., Hormazábal, E., Astudillo, A., Briceño, G., Rubilar, O., Diez, M.C., 2021. Bioconversion of potato solid waste into antifungals and biopigments using Streptomyces spp. Plos One 16 (5), 0252113. https://doi.org/10.1371/journal.pone.0252113.

Scholz, D., Kröcher, O., Vogel, F., 2018. Deactivation and regeneration of sulfonated carbon catalysts in hydrothermal reaction environments. Chem. Sus. Chem. 11, 2189–2201. https://doi.org/10.1002/cssc.201800678.

Shu, Q., Gao, J., Nawaz, Z., Liao, Y., Wang, D., Wang, J., 2010. Synthesis of biodiesel from waste vegetable oil with large amounts of free fatty acids using a carbon-based solid acid catalyst. Appl. Energy. 87, 2589–2596. https://doi.org/10.1016/j.apenergy.2010.03.024.

Song, X., Fu, X., Zhang, C., Huang, W., Zhu, Y., Yang, J., Zhang, Y., 2012. Preparation of a novel carbon-based solid acid catalyst for biodiesel production via a sustainable route. Catal. Lett. 142, 869–874. https://doi.org/10.1007/s10562-012-0840-2.

Sousa, J.A., Raposo, A., Sousa, M.M.M., Miranda, E.M., Silva, J.M.M., Magalhães, V.B., 2004. Manejo de murumuru (Astrocaryum spp.) para produção de frutos. Secretaria de Extrativismo e Produção Familiar. Rio Branco.

Thushari, I., Babel, S., 2018. Preparation of solid acid catalysts from waste biomass and their application for microwave-assisted biodiesel production from waste palm oil. Waste Manag. Res. 36, 719–728. https://doi.org/10.1177/0734242X18789821.

Wee, S.C., Maulianda, B., Harolanuar, N.H., Lee, D., Mohshim, D.F., Zaid, H.F.M., Liew, M.S., Ayoub, M.A., Elraies, K.A., Barati, R., 2019. Numerical modelling of free energy for methanol and water mixtures for biodiesel production. Fuel 55,. https://doi.org/10.1016/j.fuel.2019.115781 115781.

Xu, J., Liu, J., Ling, P., Zhang, X., Xu, K., He, L., Wang, Y., Su, S., Hu, S., Xiang, J., 2020a. Raman spectroscopy of biochar from the pyrolysis of three typical chinese biomasses: a novel method for rapidly evaluating the biochar property. Energy 202,. https://doi.org/10.1016/j.energy.2020.117644 117644.

Xu, J., Liu, J., Zhang, X., Ling, P., Xu, K., He, L., Su, S., Wang, Y., Hu, S., Xiang, J., 2020b. Chemical imaging of coal in micro-scale with Raman mapping technology. Fuel 264,. https://doi.org/10.1016/j.fuel.2019.116826 116826.

Xu, C., Nasrollahzadeh, M., Selva, M., Issaabadi, Z., Luque, R., 2019. Waste-to-wealth: biowaste valorization into valuable bio(nano)-materials. Chem. Soc. Rev. 48, 4791–4822. https://doi.org/10.1039/C8CS00543E.

Xu, J., Tang, H., Su, S., Liu, J., Xu, K., Qian, K., Wang, Y., Zhou, Y., Hu, S., Zhang, A., 2018. A study of the relationships between coal structures and combustion characteristics: the insights from micro-raman spectroscopy based on 32 kinds of chinese coals. Appl. Energy 212, 46–56. https://doi.org/10.1016/j.apenergy.2017.11.094.

Yang, W., Tang, Q., Wei, J., Ran, Y., Chai, L., Wang, H., 2016. Enhanced removal of Cd (II) and Pb (II) by composites of mesoporous carbon stabilized alumina. Appl. Surf. Sci. 369, 215–223. https://doi.org/10.1016/j.apsusc.2016.01.151.

Yu, W., Hu, J., Yu, Y., Ma, D., Gong, W., Qiu, H., Hu, Z., Gao, H., 2021. Facile preparation of sulfonated biochar for highly efficient removal of toxic Pb (II) and Cd (II) from wastewater. Sci. Total Environ. 750,. https://doi.org/10.1016/j.scitotenv.2020.141545 141545.

Zhang, B., Gao, M., Geng, J., Cheng, Y., Wang, X., Wu, C., Wang, Q., Liu, S., Cheung, S.M., 2021. Catalytic performance and deactivation mechanism of a one-step sulfonated carbon-based solid-acid catalyst in an esterification reaction. Renew. Energy 164, 824–832. https://doi.org/10.1016/j.renene.2020.09.076.

Zhao, B., O'Connor, D., Zhang, J., Peng, T., Shen, Z., Tsang, D.C.W., Hou, D., 2018. Effect of pyrolysis temperature, heating rate, and residence time on rapeseed stem derived biochar. J. Clean. Prod. 174, 977–987. https://doi.org/10.1016/j.jclepro.2017.11.013.

Zhong, Y., Zhang, P., Zhu, X., Li, H., Deng, Q., Wang, J., Zeng, Z., Zou, J., Deng, S., 2019. Highly efficient alkylation using hydrophobic sulfonic acid-functionalized biochar as a catalyst for synthesis of high-density biofuels. ACS Sustain. Chem. Eng. 7 (17), 14973–14981. https://doi.org/10.1021/acssuschemeng.9b03190.

Zhou, Y., Niu, S., Li, J., 2016. Activity of the carbon–based heterogeneous acid catalyst derived from bamboo in esterification of oleic acid with ethanol. Energy Convers. Manag. 114, 188–196. https://doi.org/10.1016/j.enconman.2016.02.027.